SCIENTIFIC REPORTS

OPEN

SUBJECT AREAS:
MICROTUBULES
CHEMOTAXIS
FILOPODIA
CELLULAR MOTILITY

Received
9 January 2013

Accepted
27 March 2013

Published
8 May 2013

Correspondence and requests for materials should be addressed to X.Y. (xyao@msm.edu) or (yaoxb@ustc.edu.cn)

* These authors contributed equally to this work.

DDA3 associates with microtubule plus ends and orchestrates microtubule dynamics and directional cell migration

Liangyu Zhang[1,2]*, Hengyi Shao[1]*, Tongge Zhu[1,2], Peng Xia[1], Zhikai Wang[1,2], Lifang Liu[4], Maomao Yan[2], Donald L. Hill[3], Guowei Fang[1], Zhengjun Chen[5], Dongmei Wang[1] & Xuebiao Yao[1,2]

[1]Anhui Key Laboratory of Cellular Dynamics and the University of Science & Technology of China, Hefei, China 230026, [2]Molecular Imaging Center, Morehouse School of Medicine, Atlanta, GA 30310, USA, [3]Comprehesive Cancer Center, University of Alabama, Birmingham, AL 35294, USA, [4]Air Force General Hospital, Beijing, China 100036, [5]Shanghai Institute of Biochemistry and Cell Biology, Shanghai, China 200031.

Cell motility and adhesion involve orchestrated interaction of microtubules (MTs) with their plus-end tracking proteins (+TIPs). However, the mechanisms underlying regulations of MT dynamics and directional cell migration are still elusive. Here, we show that DDA3-EB1 interaction orchestrates MT plus-end dynamics and facilitates directional cell migration. Biochemical characterizations reveal that DDA3 interacts with EB1 via its SxIP motif within the C-terminal Pro/Ser-rich region. Time-lapse and total internal reflection fluorescence (TIRF) microscopic assays demonstrate that DDA3 exhibits EB1-dependent, MT plus-end loading and tracking. The EB1-based loading of DDA3 is responsible for MT plus-ends stabilization at the cell cortex, which in turn orchestrates directional cell migration. Interestingly, the DDA3-EB1 interaction is potentially regulated by EB1 acetylation, which may account for physiological regulation underlying EGF-elicited cell migration. Thus, the EB1-based function of DDA3 links MT dynamics to directional cell migration.

Cell migration is necessary for various biological processes, including embryogenesis, tissue repair and regeneration, chemotaxis, and tumor metastasis. Microtubules (MTs), one of the three main types of cytoskeleton, are required for maintaining the physical properties and functional plasticity of migrating cells[1].

The plus ends of MTs, extending into the peripheral regions of cells, are dynamic, continuously switching between growing and shortening phases[2]. MT dynamics is regulated by a group of MT-associated proteins specially localized to "track" the growing MT plus ends; these are called plus-end tracking proteins (+TIPs)[3–6]. Most +TIPs bind to EB1 (end-binding protein 1) and depend on EB1 for their MT plus-end localization. They can be classified into two groups according to their EB1-binding domains. One group is +TIPs that contain a CAP-Gly domain including CLIP-115/170[7] and p150^{Glued}[8]; the other is Ser-x-Ile-Pro (SxIP) motif-containing +TIPs including APC, CLASP1/2, ACF7, STIM1, MCAK, and TIP150[4,9,10]. The conserved Ile-Pro (IP) motif was first identified in the ACF7 and APC proteins[11]. Later studies demonstrated that the SxIP motif is used by many +TIPs to bind to the end-binding homology (EBH) domain of EB1[12]. It is postulated that many +TIPs with such a motif remain to be identified and characterized.

+TIPs are involved in various cellular processes, such as MT nucleation, transport of signaling factors, MT dynamics, and stabilization[4–6]. Since the selective stabilization of MTs is essential for cell migration[1,13,14], +TIPs modulating MT plasticity and dynamics in cells are proposed to modulate factors involved in cell migration, such as CLASPs[15,16], CLIP-170[17], APC[18,19], ACF7[20], and the APC-EB1-mDia complex[21].

Cell motility is orchestrated by signaling cascades to ensure an accurate direction of migration. Although phosphorylation modulates the interaction of MTs with +TIPs[12,22], it has not been established whether other posttranslational modifications, such as acetylation, also regulate MT interaction with +TIPs during cell migration.

DDA3 (differential display activated by p53), initially identified as a down-stream target of p53[23], is thought to be involved in cell division through recruiting kif2a to spindles, and hence regulating spindle dynamics in mitosis[24]. It also participates in cell proliferation through promoting the β-catenin-mediated growth signaling pathway[25]. As DDA3 is an EB3-associated protein[25] that is frequently up-regulated in malignant peripheral nerve

sheath cells[26], it was of interest to ascertain if DDA3 is involved in EB1-interactive networks at the MT plus ends to regulate MT dynamics and hence to modulate MT-based cellular processes such as directional cell migration.

In the present effort, we demonstrated that DDA3 exhibits an EB1-dependent, MT plus-end loading and tracking. EB1 acetylation might be a mechanism of DDA3 regulation in directional cell migration. Since DDA3 is required for MT plus-ends stabilization at cell cortex, EB1-mediated loading of DDA3 to the growing plus ends of MTs may modulate MT dynamics and thereby facilitate directional cell migration.

Results

DDA3 is an EB1-binding protein. Since DDA3 is an MT-associated protein that interacts with EB3 in mouse brain[25], we speculated that DDA3 interacts with EB1 in human cells. To determine if DDA3 physically interacts with the EB1 protein, GST pull-down assays were performed using GST-EB1 as an affinity matrix to isolate His-DDA3. As shown in **Fig. 1a,** DDA3 interacted with EB1 directly. To determine if DDA3 associates with EB1 in intact cells, anti-FLAG immunoprecipitation assays were performed. Anti-GFP immunoblots confirmed that FLAG-DDA3 co-immunoprecipitates with EB1-GFP (**Fig. 1b**). Also, gel filtration analysis of HeLa cell

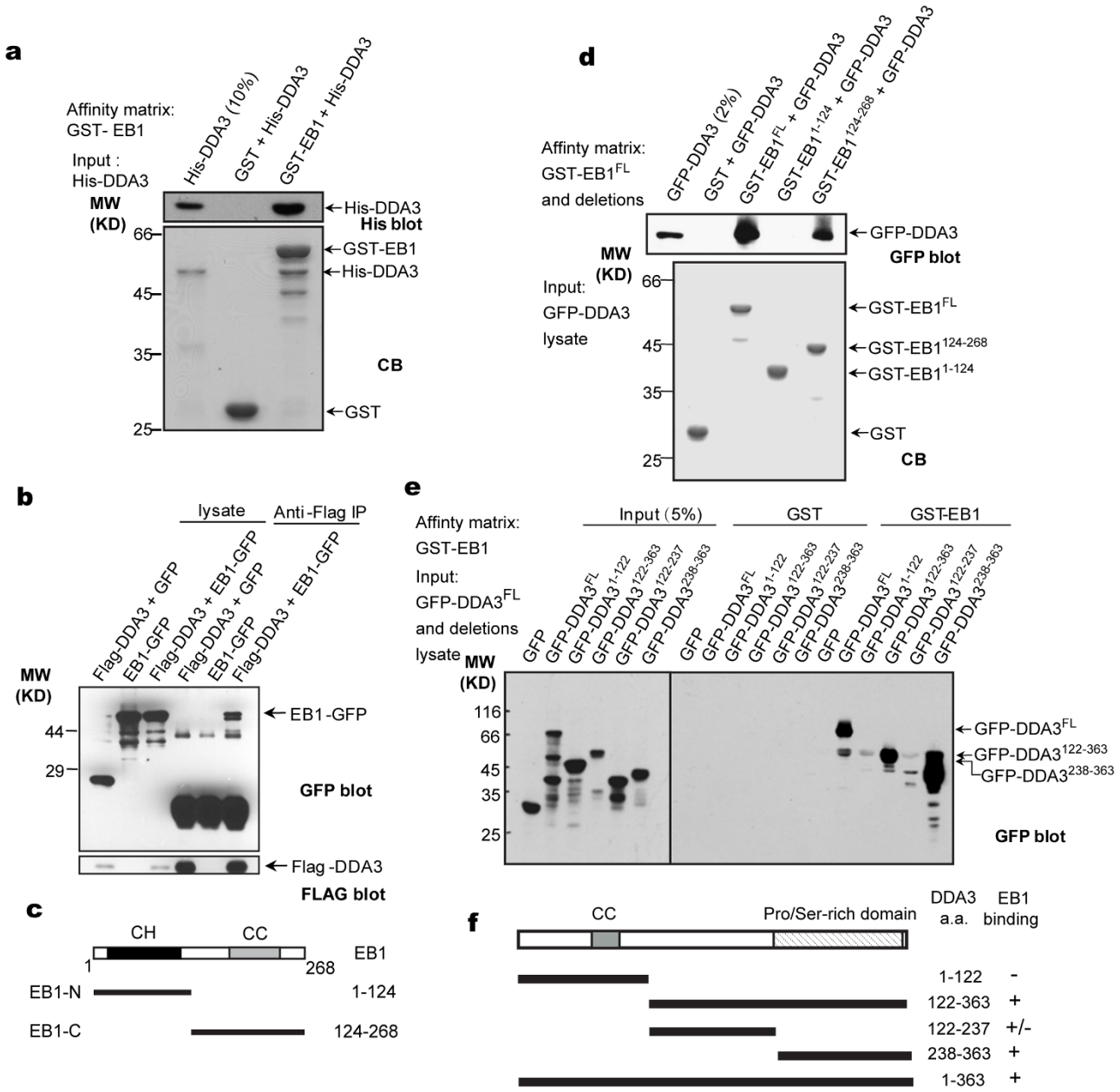

Figure 1 | DDA3 is an EB1-binding protein. (a) GST-EB1 on glutathione beads pulled down purified His-DDA3. Western blotting using anti-His antibody indicated a specific interaction. CB, Coomassie blue stain. (b) Co-immunoprecipitation of FLAG-DDA3 and EB1-GFP from human embryonic kidney 293T cells. Western blotting analysis with anti-GFP antibody indicated the specific association. (c) Schematic drawing of EB1 deletion mutants. Residue numbers at domain boundaries are indicated. CH, calponin homology domain; CC, coiled-coil region. (d) DDA3 interacted with the C-terminal domain of EB1. Purified GST-EB1 deletion mutants were used to isolate GFP-DDA3 from 293T cell lysates. Western blotting with anti-GFP antibodies showed a specific interaction. (e) DDA3 associated with EB1 via its C-terminal domain. Purified GST-EB1 was used as an affinity matrix to isolate GFP-DDA3 and its fragments from the lysates of 293T cells. Western blotting was performed as described in d. (f) Schematic representation and summary of the binding studies for a series of DDA3 deletion mutants in e. +, positive; +/−, weak; −, negative. Numbers indicate positions of the amino acid residues. CC, coiled-coil region.

extracts demonstrated the presence of DDA3 and EB1 in the same fractions (**Supplementary Fig. S1**), confirming the existence of the EB1-DDA3 complex in cells.

To map the domains for the EB1-DDA3 physical interaction, a series of EB1 and DDA3 deletion mutants were generated (**Fig. 1c, f**). As determined with a pull-down assay, GFP-DDA3 from 293T cell extracts directly bound to GST-EB1 and the GST-EB1 C terminus, consistent with other +TIPs[7,8,16,27] (**Fig. 1d**). These results indicated that DDA3 interacts with a typical +TIPs-binding domain of EB1. To delineate the domain in DDA3 responsible for EB1-binding, a GST-EB1 pull-down assay was accomplished with 293T cell extracts containing various deletion mutants of DDA3 separately. Full-length GFP-DDA3 and its two C-terminal deletion mutants, GFP-DDA3$^{122\text{-}363}$ and GFP-DDA3$^{238\text{-}363}$, were specifically absorbed by GST-EB1 (**Fig. 1e, f**), indicating that DDA3 interacts with EB1 via its C-terminus.

DDA3 is an EB1-dependent MT plus-end tracking protein. The EB1-DDA3 interaction prompted us to examine the respective patterns of subcellular distribution for these proteins. To this end, HeLa cells transfected with GFP-DDA3 were fixed and stained with corresponding antibodies. To avoid MT bundling caused by over-expression of GFP-DDA3, a preparation in which cells expressed GFP-DDA3 at a level comparable with that of endogenous DDA3 was selected (**Supplementary Fig. S2a**). Examination of the GFP-DDA3 distribution revealed a comet-like structure coinciding with that of endogenous EB1, a MT plus-end marker. Enlargement of the selected area indicated a co-distribution of DDA3 with EB1 (**Fig. 2a, upper panel**). The comet-like distribution of DDA3 at the distal plus-end of MTs was confirmed by tubulin staining in GFP-DDA3 cells (**Fig. 2a, lower panel**). Thus, in cells, GFP-DDA3 accumulates predominantly at a subset of MT-plus-ends.

If DDA3 is a +TIP, it should track the growing plus-ends of MTs. Time-lapse microscopy showed that GFP-DDA3 exhibited a typical +TIP motion in HeLa cells (**Fig. 2b, c and Supplementary Movie S1**) with an average velocity of 19.15 ± 3.37 μm/min (mean ± SD, calculated from 52 MTs in five cells). This is consistent with other +TIPs[28], suggesting that DDA3 is a +TIP. During the preparation of this work, another research group also showed that DDA3 tracks MT plus-ends in cells[29], validating our conclusion.

To define the domain responsible for the localization of DDA3 to MT plus ends, the distribution patterns of various DDA3 deletion mutants were examined in living HeLa cells. Western blotting analyses indicated that various DDA3 deletion mutants were expressed at comparable levels in these cells (**Supplementary Fig. S2b**). DDA3$^{122\text{–}363}$ and DDA3$^{238\text{–}363}$ deletion mutants co-localized with EB1 to MT plus ends in living cells (**Fig. 2d, e**). However, neither DDA3$^{1\text{–}122}$ nor DDA3$^{122\text{–}237}$ localized to the plus-ends of MTs, consistent with results in EB1-binding assays (**Fig. 1e, f**). The distribution patterns of various DDA3 deletion mutants in fixed HeLa cells (**Supplementary Fig. S2c**) were also consistent with those in living cells. Therefore, the C-terminus of DDA3 is responsible for its MT plus-end localization.

Since EB1 is a core component of protein complexes at MT plus ends, and since most +TIPs track MTs by "hitchhiking" on EB1[4,30], the interaction and co-localization of DDA3 with EB1 prompted us to determine if DDA3 tracks MT plus ends in an EB1-dependent manner. A small-hairpin RNA (shRNA) targeting the EB1 sequence was used to knock down EB1 expression in cells by transient transfection. Western blotting indicated a knockdown efficiency of at least 90% in EB1 shRNA positively-transfected cells, given that the transfection efficiency was about 70% (**Supplementary Fig. S2d, e**). An immunofluorescence assay showed that, in HeLa cells transfected with EB1 shRNA, accumulation of EB1 at MT plus ends was abolished (**Supplementary Fig. S2f**). The high performance of EB1 shRNA allowed us to establish that the mobile comets of mCherry-DDA3 were greatly reduced in EB1-suppressed HeLa cells, although a weaker MT-like distribution remained (**Fig. 2f**). In EB1-knockdown cells, the number of DDA3-labeled plus ends decreased by 66.7% along the most peripheral 100 μm^2 (**Fig. 2g**), indicating that EB1 is required for MT plus-end tracking of DDA3. As a small amount of EB3 may exist in HeLa cells[31], part of the remaining plus-end loading of DDA3 in EB1-knockdown cells may be attributed to the existence of EB3, although the contribution was much smaller compared to EB1 (**Supplementary Fig. S2g**).

To determine if MT plus-end tracking of DDA3 depends on EB1, we developed a reconstitution system to observe the behavior of DDA3 on dynamic MTs in the presence and absence of EB1. Since the GFP-DDA3 full-length protein is degraded during preparation, we selected the C-terminal domain of DDA3 (**Supplementary Fig. S2h**), a region sufficiently responsible for EB1-binding and MT plus-end tracking in intact cells (**Fig. 1e, f and Fig. 2d, e**), to examine the tracking activity of DDA3 *in vitro*. Using time-lapse total internal reflection fluorescence (TIRF) microscopy, we found that, in the presence of EB1, GFP-DDA3$^{122\text{–}363}$ labeled all growing MT plus-ends but not depolymerizing MT ends (**Fig. 2h and Supplementary Movie S2**). In contrast, without EB1, accumulation of GFP-DDA3$^{122\text{–}363}$ was almost invisible at MT growing ends (**Fig. 2i**). Statistical analysis further showed that the relative intensity of DDA3 at plus ends was decreased without EB1 (**Fig. 2j**). These results indicate that EB1 is essential for MT plus-end tracking of DDA3. Based on these results, we conclude that DDA3 is indeed an EB1-dependent +TIP.

The SxLP/SxIP motifs of DDA3 are essential for its EB1-dependent MT plus-end accumulation. The dependence of EB1 for the MT plus-end tracking of DDA3 led us to ascertain the mechanism underlying the EB1-DDA3 interaction. Previous studies showed that two motifs, the CAP-Gly domain and the Ser-x-Ile-Pro (SxIP) motif within a basic Pro/Ser-rich region, are used by other EB1-associated +TIPs[4,9]. Computational analysis revealed a conserved SxIP motif and a conserved SxLP sequence within a basic Pro/Ser-rich domain at the C-terminus of DDA3 (**Fig. 3a**). Since the C-terminal region of DDA3 is responsible for its EB1 binding (**Fig. 1e, f**) and MT plus-end tracking (**Fig. 2**), it appeared likely that DDA3 binds to EB1 via these SxLP/SxIP motifs.

To assess this hypothesis, we replaced the hydrophobic Leu-Pro dipeptide (Leu277, Pro278) and Ile-Pro dipeptide (Ile283 and Pro284) of DDA3 individually or simultaneously with the residues Asn-Asn and analyzed the resulting proteins for interaction with EB1 using GST pull-down assays and for their distribution in cells using fluorescence microscopy. Substitution of the residues eliminated the interaction of DDA3 with EB1 (**Fig. 3b, c**) as well as MT tip accumulation of DDA3, as determined in living cells (**Fig. 3d**) and fixed cells (**Supplementary Fig. S3b**). To avoid the potential difference of expression levels of GFP-DDA3 and its mutants, preparations in which the levels of GFP-DDA3 and its mutants were comparable were selected (**Supplementary Fig. S3a**). Replacement of Ile-Pro residues with Asn-Asn alone (GFP-DDA3$^{IP\text{-}NN}$) decreased the binding activity with EB1 and the MT plus-end localization of DDA3 to greater extents than that of substitution of Leu-Pro with Asn-Asn alone (GFP-DDA3$^{LP\text{-}NN}$) (**Fig. 3b–d and Supplementary Fig. S3b**). Simultaneous replacement of Leu-Pro and Ile-Pro dipeptides (GFP-DDA3$^{LPIP\text{-}NNNN}$) abolished the binding with EB1, as determined in pull-down assays (**Fig. 3b, c**), and essentially eliminated the MT plus-end accumulation of DDA3 in cells (**Fig. 3d and Supplementary Fig. S3b**).

To determine if SxLP/SxIP motifs are essential for the MT plus-end tracking of DDA3 *in vitro*, a TIRF microscopy assay was performed. In the presence of EB1, GFP-DDA3$^{122\text{–}363}$ tracked the growing ends of MTs (**Fig. 3e and Supplementary Fig. S3c**). In contrast, almost no accumulation of GFP-DDA3$^{122\text{–}363\ LPIP\text{-}NNNN}$ was visible at MT growing ends under the same conditions (**Fig. 3f**). The

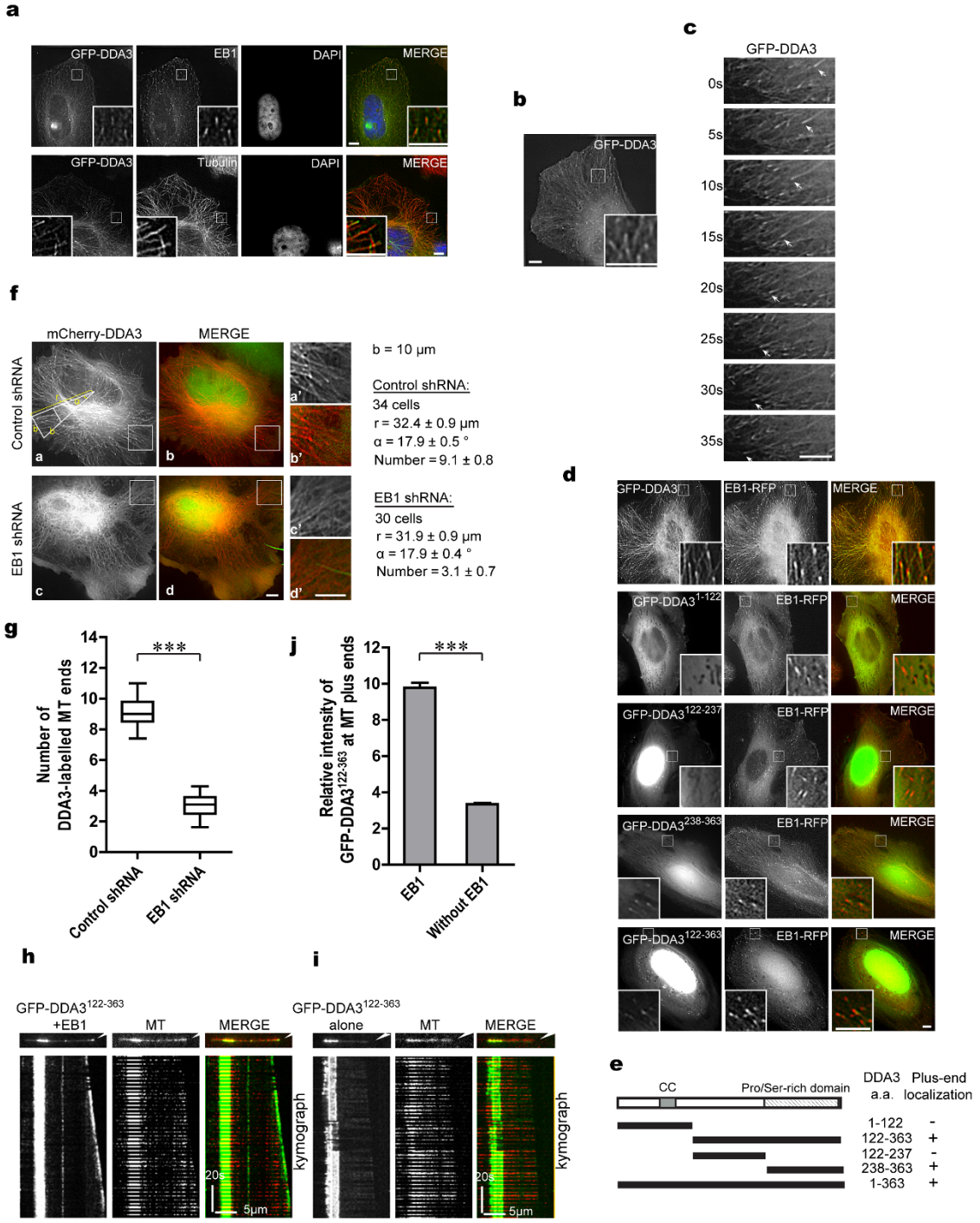

Figure 2 | DDA3 is an EB1-dependent MT plus-end tracking protein. (a) As determined with fixed cells, DDA3 co-localized with EB1 at MT plus ends. HeLa cells were transiently transfected with GFP-DDA3 (green), fixed, and then labeled with antibodies against EB1 (red) or tubulin (red). 4′,6-Diamidino-2-phenylindole (DAPI; blue) was used for DNA staining. (b) DDA3 localized to MT plus ends in live cells (see Supplementary Movie S1). (c) DDA3 tracked MT plus ends in live cells. Arrows indicate that GFP-DDA3 associates with the growing MT plus ends. (d) Live-cell images of HeLa cells co-transfected with EB1-RFP and a series of DDA3 deletion mutants. (e) Schematic representation and summary of the localization studies for various DDA3 deletion mutants in d. +, positive; −, negative. Numbers indicate positions of the amino acid residues. (f) Live-cell images of HeLa cells co-transfected with mCherry-DDA3 (red) and EB1 shRNA (green) or control shRNA (green). (g) Statistical analysis of MT plus-end localization of DDA3 in control and EB1-suppressed cells. For HeLa cells at 72 hr post-transfection, numbers of mCherry-DDA3-positive comets were measured in a trapezoid part of the cell sector (approximately 100 μm^2, with a base *b*, along the most peripheral 10 μm as shown in f). Approximately 30 cells were analyzed for each condition in three independent experiments. ***, $P < 0.001$ by t-test. (h) TIRF experiments indicated that $DDA3^{122–363}$ tracks the growing MT plus-ends in the presence of EB1. The corresponding kymograph at the bottom shows the same MT over a period of 2 min. (See Supplementary Movie S2). (i) In the absence of EB1, the MT plus-end tracking of DDA3 was almost undetectable. (j) Statistical analysis of the relative intensities of $DDA3^{122–363}$ at MT plus ends in h and i. The relative intensity of $DDA3^{122–363}$ at plus ends is the ratio of average intensity in a circle of 5 pixels at the plus end divided by the average intensity at the lattice within a region of the same size. Data are presented as means ± SEM from three independent experiments. ***, $P < 0.001$ by t-test. Scale bars, 5 μm (all image panels).

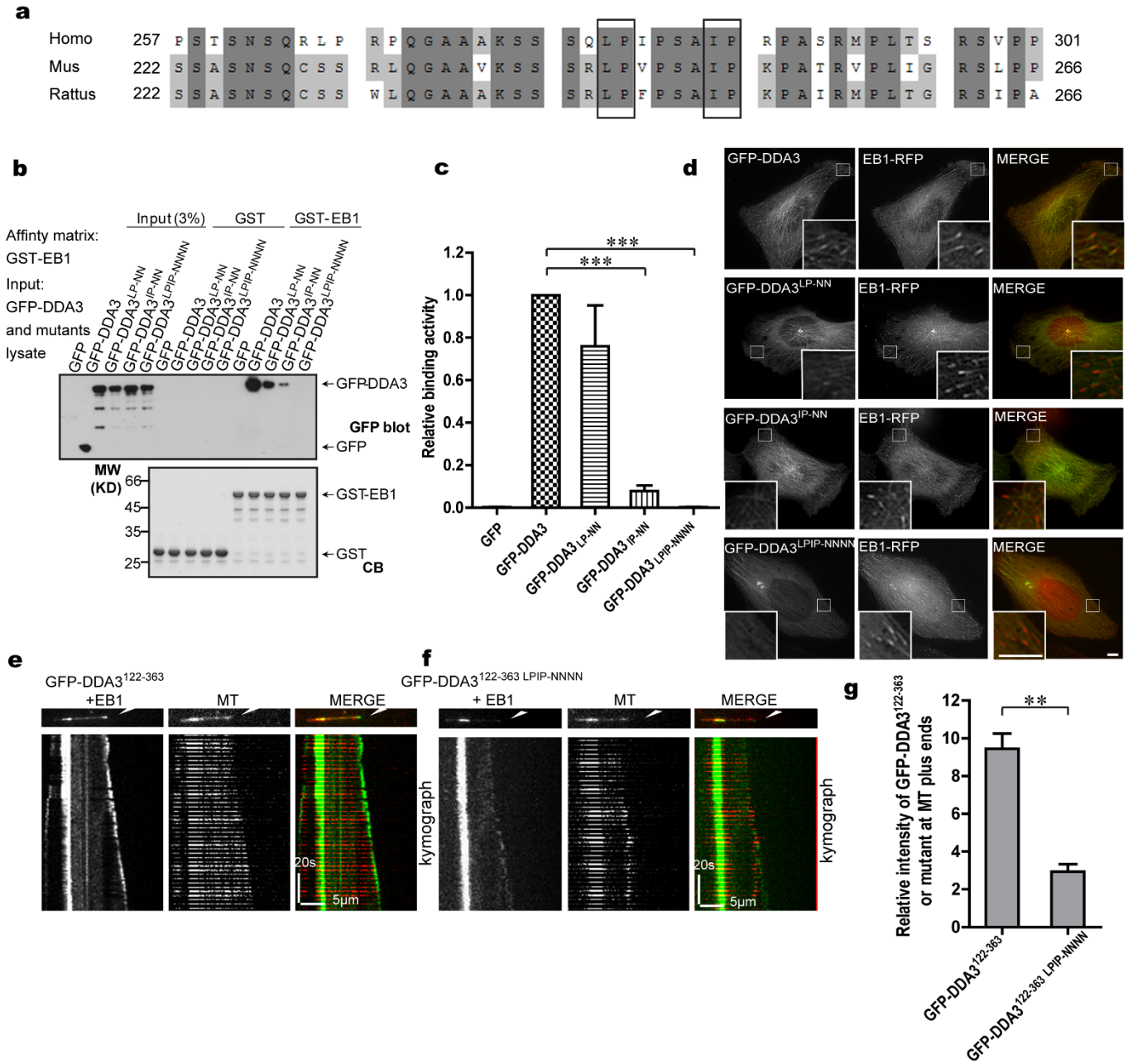

Figure 3 | The SxLP/SxIP motifs of DDA3 are essential for its EB1-dependent MT plus-end accumulation and tracking. (a) Shown is the sequence alignment of the basic Pro/Ser-rich regions in DDA3 from human (*Homo*), mouse (*Mus*), and rat (*Rattus*). Dark and light shading indicate the identical and conserved residues, respectively. The residues in the black squares indicate the potential EB1-binding motifs. Numbers indicate the amino acid positions. (b, c) SxLP/SxIP motifs are essential for DDA3-EB1 binding *in vitro*. (b) GST-EB1 was used as an affinity matrix to isolate various GFP-DDA3 mutants from 293T cell extracts, followed by Western blotting analysis with GFP antibody to indicate the specific interaction. (c) Quantitative analysis of the relative binding activity in b. The ratio of GFP-DDA3/GST-EB1 was normalized to 1 in each experiment. Data are presented as means ± SD from three independent experiments. ***, $P < 0.001$ by t-test. (d) SxLP/SxIP motifs are essential for the plus-end accumulation of DDA3 in cells. Shown is live imaging of HeLa cells transiently co-transfected with EB1-RFP (red) and the indicated GFP-DDA3 mutants (green). (e, f) TIRF experiments indicated that SxIP/SxLP motifs are essential for the EB1-dependent MT plus-end tracking of DDA3$^{122–363}$ *in vitro*. The corresponding kymograph at the bottom shows the same MT over a period of 2 min. (g) Statistical analysis of the relative intensity of DDA3$^{122–363}$ at MT plus ends in e and f, as described in Fig. 2j. **, $P < 0.01$ by t-test. Scale bars, 5 μm (all image panels).

relative intensity of the DDA3 mutant at plus ends was decreased compared with wide-type DDA3 (**Fig. 3g**). These results indicated that SxLP/SxIP motifs are essential for the EB1-dependent tracking of DDA3. Based on these results, we conclude that the SxLP/SxIP motifs in DDA3 mediate its EB1-dependent MT plus-end tracking.

DDA3 modulates MT plus-end dynamics in the region of cell cortex. Although they co-localize to the distal plus ends of MTs, +TIPs may have different effects on MT dynamics[4]. The +TIP property of DDA3 led us to examine its potential functions in MT dynamics. To this end, an shRNA specifically targeting the non-coding region of DDA3 gene was constructed to knock down DDA3 expression in HeLa cells. In those positively transfected ells, the knockdown efficiency was at least 90%, considering that the transfection efficiency was about 60% (**Supplementary Fig. S4a, b**). The roles of DDA3 on MT plus-end dynamics in HeLa cells

were then examined with EB3-mCherry as a MT plus-end marker. As shown in **supplementary Fig. S4c**, the average MT polymerization rate was 32.5% faster (17.68 ± 0.11 μm/min) in DDA3-knockdown cells than that in control cells (13.34 ± 0.08 μm/min). These data indicate that DDA3 may be responsible for decreasing the MT polymerization rate and promoting MT plus-end stabilization.

As MT plus-end dynamics in the cell cortex region are involved in cell morphogenesis, polarity, and migration, we focused on the role of DDA3 on MT plus-end dynamics in this region. To avoid the potential influence of over-expressed EB3-mCherry on MT dynamics, cells expressing mCherry-tubulin were used. DDA3 knockdown increased the unstable MT ends in the cell cortex region (**Fig. 4a and Supplementary movie S3**). For statistical analysis of the MT dynamics, kymographs of the MT plus ends in DDA3-knockdown and control cells were made (**Fig. 4b and Supplementary Fig. S4d–f**). In DDA3-depleted cells, the MT growth rate

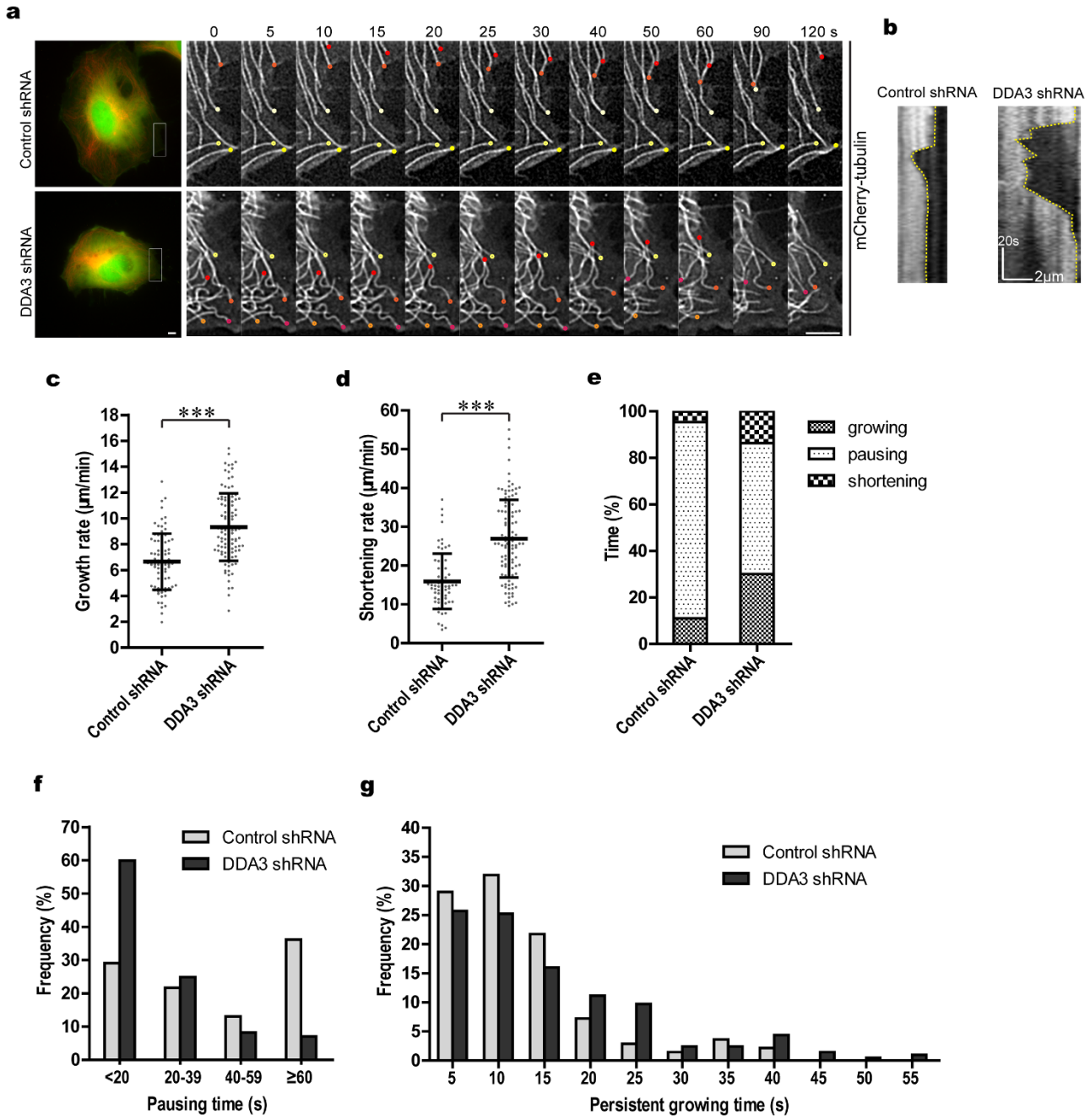

Figure 4 | DDA3 is required for MT plus-ends stabilization in the region of cell cortex. (a) Time-lapse images show the MT plus-end dynamics in DDA3-knockdown cells. HeLa cells were co-transfected with mCherry-α-tubulin (red) and control or DDA3 shRNAs (green) for 72 hr, and then live-cell images were collected at 1-sec intervals. Red dots indicate relatively dynamic ends; yellow dots indicate relatively stable ends (See Supplementary Movie S3). (b) Kymographs showing plus-end dynamics of two MTs from control or DDA3 shRNA-treated cells in a period of 2 min. (c, d) Statistical analysis of MT growth rate and shortening rate at the cell cortex in a. Data are presented as means ± SD and are derived from approximately 100 MTs in 20 cells from three independent experiments. ***, $P < 0.001$ by t-test. (e) The percentages of growing, pausing, and shortening times that MTs displayed at the cell cortex in a. Data are derived from approximately 150 MTs in 20 cells from three independent experiments. (f, g) Frequencies of MT persistent pausing or persistent growing at the cell cortex in a. Data are derived from approximately 150 MTs in 20 cells from three independent experiments. Scale bars, 5 μm (a), 2 μm (b). See also Supplementary Table S1.

and shortening rate increased by 40.2% and 70.9%, respectively, relative to that in control cells (**Fig. 4c, d and Supplementary Table S1**). At the cortex of DDA3-knockdown cells, MT plus-ends displayed less time in pausing, but longer time in growing and shortening (**Fig. 4e and Supplementary Table S1**). Further, DDA3 suppression resulted in an increased frequency of MT persistent growth, but a decreased frequency of MT persistent pausing (**Fig. 4f, g and Supplementary Table S1**). Therefore, DDA3 depletion reduced MT pausing and increased MT dynamics at the cell cortex. Further investigation indicated that DDA3 knockdown led to an increase in the frequency of MT catastrophe by 1.84 times and a reduction of MT rescue frequency by 0.35 times relative to the controls (**Supplementary Table S1**). These data suggest DDA3 may be responsible for MT stabilization in the cell cortex region.

DDA3 is essential for directionally persistent cell migration. To modulate cell migration, several +TIPs that regulate MT stability and dynamics have been proposed. These include CLASPs[15,16], APC[18,19], CLIP-170[17], ACF7[20], and the APC-EB1-mDia complex[21]. The characteristics of DDA3 on regulation of MT dynamics indicated a role for this protein in cell migration. To validate this hypothesis, a small interfering RNA (siRNA) was used to knock down the expression of DDA3 in MDA-MB-231 cells. Western blotting revealed that DDA3 was efficiently depleted by the specific siRNA but not by scrambled sequences (**Supplementary Fig. S5**). As previous studies showed that EB1 is involved in cell migration[21], we used EB1 as a positive control. In wound healing assays, knockdown of EB1 and DDA3 individually or simultaneously decreased the relative migration velocities of cells toward the opposite side by 54.4%, 61.9%, and 69.1%, respectively, compared to that of the scrambled siRNA control (**Fig. 5a, b**). These results indicate directional migration defects in DDA3-depleted cells.

To investigate the mechanisms underlying these defects in DDA3-suppresed cells, migration of single cells was examined. MDA-MB-231 cells transfected with control shRNA (green) or DDA3 shRNA (green) were starved and then stimulated by serum to migrate. Suppression of DDA3 resulted in defects of directionally persistent cell migration (**Fig. 5c and Supplementary movie S4**). The migration velocity (V_T) and directional migration velocity (V_D) of MDA-MB-231cells were calculated (**Fig. 5d**). The V_T of DDA3-suppressed cells was similar to that of control shRNA-transfected cells, compared to that of the surrounding non-transfected cells (**Fig. 5e and Supplementary Table S2**); in contrast, V_D was reduced in DDA3-suppressed cells, indicating that DDA3 functions in directionally persistent migration of MDA-MB-231 cells (**Fig. 5f and Supplementary Table S2**). Thus, we conclude that DDA3 is required for directionally persistent migration of MDA-MB-231 cells.

EB1-DDA3 interaction is potentially regulated by acetylation underlying directional cell migration. Recruitment of DDA3 to MT plus-ends by EB1 involves in promoting MT plus-end stabilization at the cell cortex, which in turn facilitates directionally persistent cell migration. The DDA3-EB1 interaction, however, should be regulated to orchestrate these cellular processes. As our previous findings revealed that EB1 acetylation at K220 by PCAF facilitates normal mitotic progression by regulating interactions of EB1 with a variety of +TIPs containing the SxIP motif[32], we hypothesized that acetylation of EB1 may also regulates the interaction of DDA3 with EB1 and hence modulates the MT plus-end loading and tracking of DDA3.

To examine if acetylation of EB1 modulates its interaction with DDA3, we used GST-DDA3 as affinity matrix to pull down EB1 and in vitro biochemically acetylated EB1. As shown in **Fig. 6a**, GST-DDA3 pulled down EB1 (**upper panel**) but not EB1 acetylated at K220 (**middle panel**), indicating that acetylation of EB1 at K220 might inhibit the DDA3-EB1 interaction. Since the acetylation of EB1 at K220 by PCAF in vitro never achieved 100%, a portion of non-acetylated EB1 was absorbed by GST-DDA3 affinity beads (**lane 6, upper panel**). To further validate our findings, we replaced the Lys220 of EB1 with Arg (K220R, a non-acetylatable mutant) or Gln (K220Q, an acetylation-mimicking mutant) and used GST-DDA3 to pull down EB1 and its K220 mutants. Consistent with our previous results[32], The acetyl-mimetic mutation of EB1 ($EB1^{K220Q}$) abolished the interaction of EB1 and DDA3 (**Supplementary Fig. S6a**). The $EB1^{K220R}$ mutant, instead of mimicking a non-acetylatable mutant, significantly attenuated DDA3-EB1 binding but did not abolish it (**Supplementary Fig. S6a**). The reason for this effect may be that K220 stabilizes the hydrophobic cavity in the EB1 EBH domain and that K220R may perturb such a cavity by disrupting the corresponding hydrogen bonds[32]. Thus, the EB1 K220 is critical for EB1-DDA3 interaction underlying cell migration.

To determine the effects of EB1 acetylation at K220 on MT plus-end tracking of DDA3 in cells, EB1-GFP or $EB1^{K220Q}$-GFP was added back into EB1-knockdown cells to evaluate their rescue effects on the MT plus-end tracking of DDA3. Although EB1 and $EB1^{K220Q}$ tracked MT plus-ends (**Fig. 6b**), EB1 but not $EB1^{K220Q}$ rescued the plus-end tracking of DDA3 in cells with endogenous EB1-knockdown (**Fig. 6b, c**). Thus, in cells, acetylation of EB1 at K220 may inhibit MT plus-end tracking of DDA3.

TIRF microscopy was used to determine if EB1 acetylation at K220 also regulated the MT plus-end tracking of DDA3 *in vitro*. As shown in **Fig. 6d–f**, GFP-$DDA3^{122–363}$ accumulated at the growing plus ends of MTs in the presence of EB1 but not $EB1^{K220Q}$. Since the MT plus-end tracking activities of EB1 and $EB1^{K220Q}$ were comparable *in vitro* (**Supplementary Fig. S6b–d**), the inhibition of MT plus-end tracking of DDA3 by $EB1^{K220Q}$ is due mainly to the perturbation of DDA3-EB1 interaction by mutation of critical K220.

To examine whether EB1 acetylation exhibits any physiological regulation in cell migration, EB1 acetylation at K220 in DDA3-mediated migrating cells was evaluated. MDA-MB-231 cells were starved and then stimulated by serum to migrate. Serum stimulation of 10 min significantly increased the level of EB1 K220 acetylation (**Supplementary Fig. S6e, f**). We then determined the potential function of EB1 acetylation in cell migration. MDA-MB-231 cells co-transfected with EB1 shRNA (green) and EB1-RFP or $EB1^{K220Q}$-RFP (red) were starved and then stimulated by serum to migrate. The migration of single cells was examined. EB1, but not $EB1^{K220Q}$, rescued the directionally persistent migration in cells with endogenous EB1 suppression (**Supplementary Fig. S6g**). Although there was no difference in migration velocity between EB1- and $EB1^{K220Q}$-add-back cells (**Supplementary Fig. S6h and Supplementary Table S3**), the directional migration velocity of $EB1^{K220Q}$-add-back cells was extremely lower than that of EB1-add-back cells (**Supplementary Fig. S6i and Supplementary Table S3**), compared to the surrounding non-transfected cells. These results suggest that dynamic acetylation of EB1 at K220 may participate in directional migration of MDA-MB-231 cells. Based on these results, we reason that EB1 acetylation might be a potential mechanism underlying directional cell migration.

Discussion

Spatial control of cell migration is critical to developmental morphogenesis, tissue homeostasis, and tumor metastasis. Cell senses gradients of extracellular cues to orchestrate the directional movements. The MT plus-end-tracking proteins establish a complex structure platform that serves as a molecular engine to regulate MT dynamics and thereby orchestrates cellular events such as cell migration. However, the regulatory mechanisms underlying the MT dynamics and directional cell movement have remained elusive. We used high-resolution time-lapse TIRFM to demonstrate that DDA3 exhibits EB1-dependent MT plus-end tracking. It interacts with the EBH domain of EB1 through its conserved SxLP/SxIP motifs. Recruitment of DDA3 to MT plus-ends by EB1 promotes MT plus-end

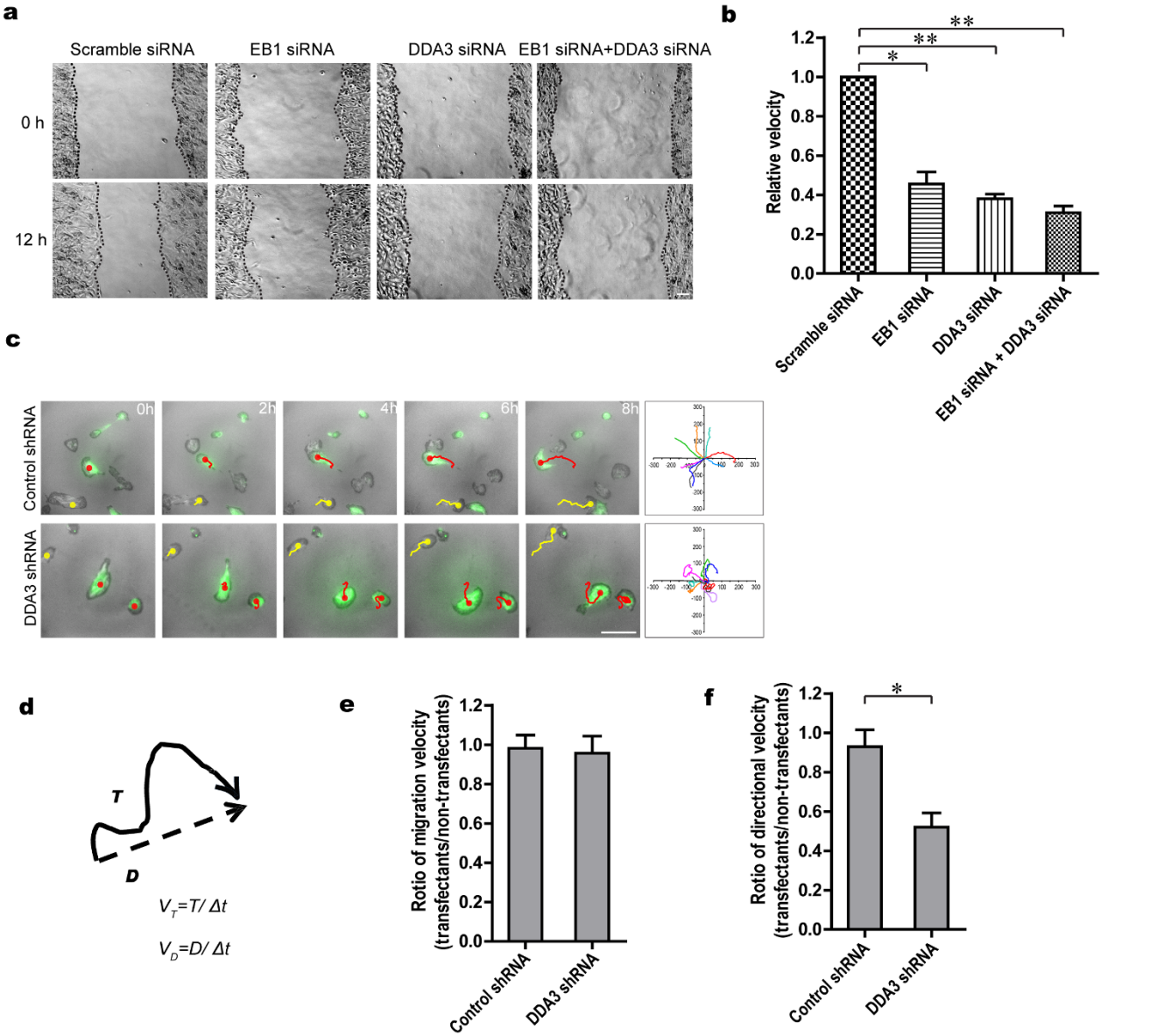

Figure 5 | DDA3 is essential for directionally persistent cell migration. (a, b) In MDA-MB-231 cells, suppression of DDA3 or EB1 caused defects in directional migration. (a) Cells were treated with indicated siRNAs for 72 hr and then were wounded, followed by visualization by phase contrast microscopy at indicated times. (b) Quantitative analysis of relative migration velocities of cells toward the opposite side in a. Data are presented as means ± SEM from three independent assays. *, $P < 0.05$; **, $P < 0.01$ by t-test. (c–f) Suppression of DDA3 resulted in defects in directionally persistent cell migration. (c) MDA-MB-231 cells transfected with control or DDA3 shRNAs (green) were treated as described in 'Materials and Methods' and then imaged at 10-min intervals (See Supplementary Movie S4). Migration tracks of transfectants and non-transfectants are shown as red and yellow lines, respectively. The tracks of eight randomly picked transfected cells are presented for each group. (d) Diagram of migration velocity (V_T) and directional migration velocity (V_D) calculation of a cell. V_T is the ratio of total track distance to total time. V_D is the ratio of direct distance from start to end point to total time. (e) Migration velocities of control shRNA-transfected cells, DDA3 shRNA-transfected cells and non-transfected cells were evaluated. The ratio of migration velocity of DDA3 shRNA-transfected cells ($V_{T\text{-}DDA3shRNA}$) to that of non-transfected cells ($V_{T\text{-}non}$) was used to reflect the effects of DDA3-knockdown. (f) Directional migration velocities of control shRNA-transfected cells, DDA3 shRNA-transfected cells and non-transfected cells were evaluated. The ratio of directional migration velocity of DDA3 shRNA-transfected cells ($V_{D\text{-}DDA3shRNA}$) to that of non-transfected cells ($V_{D\text{-}non}$) was used to reflect the effects of DDA3-knockdown. Data are presented as means ± SEM from at least 60 cells for each condition from three independent experiments. *, $P < 0.05$ by t-test. Scale bars, 100 μm (all image panels).

stabilization at the cell cortex, which in turn facilitates directional cell movement. In addition, PCAF-mediated acetylation of EB1 may be a potential mechanism of DDA3 regulation in EGF-elicited migrating cells. Based on those studies, we reason that the dynamic interaction of DDA3 with EB1 orchestrates MT dynamics underlying directional cell migration (**Supplementary Fig. S6j**).

DDA3 was previously shown to be an EB3-binding protein, but whether DDA3 exhibits any MT plus-end tracking activity and how this tracking is regulated have remained elusive[25]. Since EB1 is a major isoform among three EB proteins in mammalian cells and EB1 exhibits similar structural feature for binding +TIPs like that in EB3, we sought to examine how DDA3 binds to EB1 and functions as a unique +TIP during cell migration. During the preparation of this work, Jiang et al. reports their finding that DDA3 binds to EB1 in reconstituted system[29], which is consistent with our characterization. However, their study did not address the functional relevance of

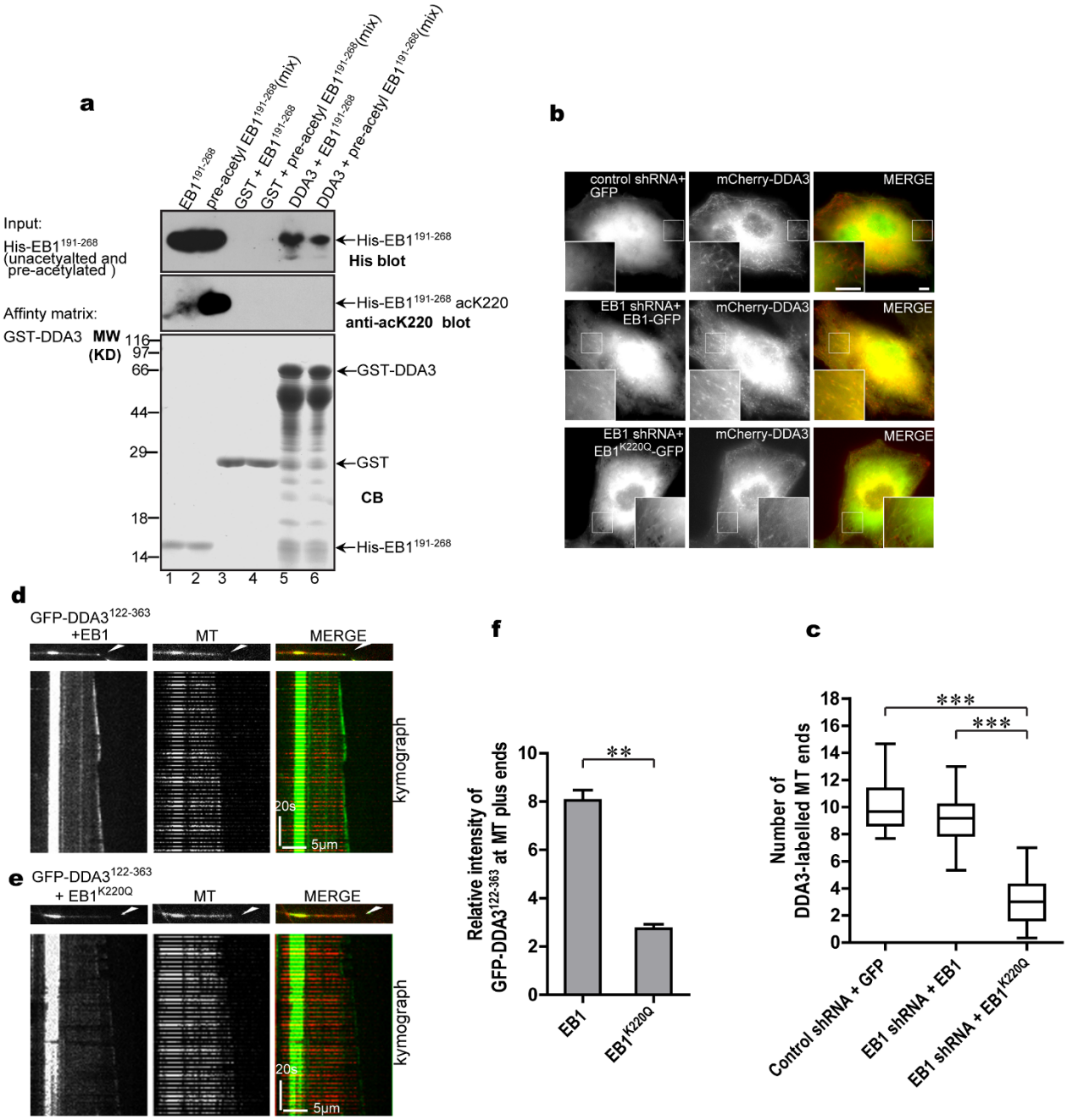

Figure 6 | EB1 acetylation at K220 may regulate the MT plus-end loading and tracking of DDA3. (a) Acetylation of EB1 at K220 inhibited DDA3-EB1 interaction. GST-DDA3 was used as affinity matrix to pull down His-EB1$^{191–268}$ and pre-acetylation-treated His-EB1$^{191–268}$. Western blotting analyses were then performed with His antibody and anti-acK220 antibody to indicate specific interaction. (b) EB1^{K220Q} inhibited MT plus-end tracking of DDA3 in cells. HeLa cells were co-transfected with mCherry-DDA3, EB1 shRNA, and EB1-GFP or its mutant for 72 hr, and then live cell images were collected. (c) Statistical analysis of MT plus-end localization of mCherry-DDA3 in b, as described in Fig. 2g. ***, $P < 0.001$ by t-test. (d, e) TIRF experiments, performed *in vitro*, indicated that EB1^{K220Q} inhibits MT plus-end tracking of DDA3. The corresponding kymograph at the bottom shows the same MT in a period of 2 min. (f) Statistical analysis of the relative intensity of DDA3$^{122–363}$ at MT plus ends in d and e, as described in Fig. 2j. **, $P < 0.01$ by t-test. Scale bars, 5 μm (all image panels).

DDA3 in cellular dynamics. Our study showed that DDA3 depends on EB1 for its MT plus-end localization and tracking (**Fig. 2**) using a characteristic "hitchhiking" mechanism for plus-end targeting[4]. Importantly, our study revealed that DDA3 interaction with EB1 might be regulated by acetylation during cell migration.

Our early computational analyses predict that DDA3 exhibits a typical EB1-binding motif, suggesting that DDA3 is a unique +TIP[33]. Indeed, DDA3 binds to EB1 via its two conserved motifs, the SxLP motif and an SxIP motif within a basic Pro/Ser-rich region at the C-terminus of DDA3 (**Fig. 3**). Interestingly, the contributions of these two motifs to EB1-binding and MT plus-end localization of DDA3 are different (**Fig. 3b–d**). Since the amino acids in the SxIP motif and its surrounding sequence are essential for EB1 binding[34], the different binding affinity may be attributed to the unique sequence of each motif. DDA3 contains an unfavorable Ala residue at the x-position of SxIP. Its surrounding sequence, however, is rich in favorable residues. Thus, the SxIP motif is more essential for DDA3-EB1 binding. The SQLP motif in DDA3 is a newly identified

site for EB1 binding. Although its flanking regions are enriched in favorable residues, it contains two unfavorable residues, Gln and Leu, in the SQLP motif, which reduces its EB1-binding affinity relative to that of the SAIP motif. It would be of great interest to examine whether two EB1-binding motifs in DDA3 exhibit synergistic action toward the EB1-binding and how those two sites are regulated during cell migration. It is worth-noting that phosphorylations in the vicinity of the SxIP motif negatively regulate the MT plus-end tracking activities of +TIPs by decreasing their EB1-binding capacities[4,11,22,35]. Since there are several serines in the vicinity of the SxLP/SxIP motifs in DDA3, it would be of equal importance to characterize and elucidate the spatiotemporal control of DDA3 by potential acetylation-phosphorylation cross-talk in stationary and migratory cells.

Through analysis of the kinetic parameters of MT polymerization in DDA3-depleted cells, DDA3 was shown to be involved in promoting MT plus-end stabilization at the cell cortex (**Fig. 4**). A previous study revealed that the C-terminus of DDA3 promotes MT polymerization *in vitro*[25]. In the present effort, DDA3 was indicated to be involved in MT plus-end stabilization via inhibiting MT catastrophe and promoting MT pause and rescue in cells. Thus, the property of DDA3 in stimulating MT polymerization *in vitro* is probably due to its activity of inhibiting MT catastrophe and promoting MT rescue. Since selective stabilization of MTs is essential for cell migration[1,13,14], DDA3 is likely involved in this process by promoting MT stabilization. Further investigation of intrinsic cell motility revealed that DDA3 has no effect on the total migration velocity of MDA-MB-231 cells but is essential for their directionally persistent migration (**Fig. 5**). Thus, the excitement and challenge ahead are to elucidate the structural basis of DDA3 interaction with EB1. The structural basis of this interaction will enable us to consolidate the EB1-DDA3 interaction and regulation into a mechanistic model by which DDA3 operates the EGF-elicited directional movements.

During cell migration, the accumulation of +TIPs at MT plus-ends facilitates MT search and capture, which, in turn leads to their capture by specific targets at the cell cortex[14,36,37]. The promotion of MT plus-end pause and reduction of MT plus-end dynamics at the cell cortex by DDA3 also indicate that DDA3 promotes the connection between MT plus-ends and cell cortical proteins to facilitate cell polarization and migration, similar to that of EB1[21], CLIP170[17], APC[38], and CLASPs[39–41]. By use of anti-FLAG DDA3 immunoprecipitation combined with mass spectrometry, we identified IQGAP1 as a DDA3-interacting protein at the cell cortex (Zhang et al., unpublished observation), indicating a potential linkage between MT and leading edge cortex.

Although the selective stabilization of MTs at the cell cortex is essential for cell migration, the MT plus-ends should be dynamically regulated to ensure directionally persistent cell migration. Our study suggested that acetylation of EB1 may regulate DDA3-EB1 interaction and serve as a new regulation mechanism underlying directional cell migration (**Fig. 6**). Since acetylation of EB1 at K220 destabilizes the hydrophobic cavity responsible for EB1-SxIP interaction[32], we propose that acetylation of EB1 modulates the interaction of EB1 with most +TIPs containing an SxIP motif and that DDA3 is important for directional migration of cells. Goh et al., recently reported that EGF stimulation elicits EGFR acetylation underlying EGFR endocytosis[42]. It would be of great importance to test whether PCAF is responsible for EGFR acetylation and whether the acetylation regulates EGFR kinase activity and/or kinetics in localization to the leading edge of migrating cells. It is worth noting that BRCA2 is responsible for localizing of PCAF in nuclear structures and BRCA2 null breast cancer patients exhibit high level of cytoplasmic PCAF and invasive phenotype in clinic oncology[43]. Given the fact that PCAF may orchestrates EB1-DDA3 interaction in directional migration, it would be of great clinic relevance to test if EB1 acetylation level is altered in the aforementioned BRCA2 null breast cancer patients and whether interrogation of EB1-DDA3 interaction and interaction of EB1 with other potential +TIPs could attenuate BRCA2 null breast cancer invasiveness and metastasis.

In summary, our findings reveal that DDA3 exhibits an EB1-dependent, MT plus-end tracking. EB1-mediated loading of DDA3 to the growing plus-ends of MTs modulate MT dynamics and thereby facilitate directional cell migration. PCAF-mediated EB1 acetylation may serve as a potential mechanism of DDA3 regulation in EGF-elicited migrating cells. The potential regulation of DDA3 by EB1 acetylation provides a unifying view of the regulation pathways underlying +TIPs in directional cell migration. This mechanistic interaction of EB1-DDA3 established here now allows investigations of the upstream signaling transduction pathways underlying direction cell migration and tumor metastasis.

Methods

Cell culture and transfection. Cells were purchased from American Type Culture Collection (Manassas, VA, USA). HeLa cells and 293T cells were cultured in DMEM (Invitrogen, Carlsbad, USA) containing 10% fetal bovine serum (FBS, Hyclone, Logan, UT) and 1% glutamine at 37°C with 8% CO_2. MDA-MB-231 cells were maintained in L-15 medium containing 10% FBS at 37°C. Cells were transfected with plasmids or siRNAs using Lipofectamine 2000 (Invitrogen), according to manuals from the manufacturers.

Antibodies and siRNA. Anti-DDA3 antibody was generated by immunizing mice with purified recombinant DDA3 proteins from bacterial cells. Anti-EB1 acetyl-K220 antibody was developed as described previously[32]. The following antibodies were obtained from commercial sources: anti-EB1 mouse antibody (BD Biosciences, Palo Alto, CA); anti-GFP antibody (BD Biosciences); anti-FLAG (M2) antibody (Sigma); and anti-α-tubulin antibody DM1A (Sigma).

EB1 siRNA (5′-AAGUGAAAUUCCAAGCUAAGC-3′) was synthesized by Qiagen (USA)[32]. DDA3 siRNA targeting the 3′ non-coding sequence AAGCAAGACUUCAGUAGCAUU was synthesized by Dharmacon (Boulder, CO, USA) as described previously[24]. The small-hairpin RNAs (shRNA) against EB1 and DDA3 were constructed using the same targeting sequences as their siRNAs. The pLKO.1-GFP vector was used as control. All the siRNAs and shRNAs were transfected into cells using Lipofectamine 2000 (Invitrogen) for 48 or 72 hr, and knockdown efficiencies were confirmed by Western blotting and/or immunofluorescence.

***In vitro* pull-down assay.** Pull-down assays were performed as described previously[44]. Briefly, GST fusion protein-bound Sepharose beads were incubated with human embryonic kidney 293T cell lysates containing ectopically-expressed GFP-tagged proteins or their deletion mutants or with purified His-tagged fusion proteins expressed in bacterial cells. Proteins on beads were then boiled in the SDS sample buffer and subjected to immunoblotting.

***In vitro* acetylation.** The detailed biochemical characterization of EB1 acetylation *in vitro* was recently described[32]. Briefly, recombinant $PCAF^{352–832}$ and EB1 or its mutants were incubated in HAT buffer (250 mM Tris·HCl, pH 8.0; 50% (vol/vol) glycerol; 0.5 mM EDTA; and 5 mM DTT) in the presence of 1 mM acetyl-CoA (Sigma; A2056) at 30°C for 1.5 hr.

Immunofluorescence and live cell images. Cells were seeded onto sterile, acid-treated 12-mm coverslips in 24-well plates (Corning Glass Works, Coring, NY) for transfection or drug treatment[45]. For visualization of +TIPs and MTs, cells were fixed with cold methanol for 5 min at −20°C. After washing three times with PBST (0.05% Tween-20 in PBS), cells were blocked with 1% bovine serum albumin (Sigma) for 45 min at room temperature. Cells were subsequently incubated with primary antibodies in a humidified chamber for 1 hr at room temperature, followed by secondary antibodies for 1 hr at room temperature. DNA was stained with 4′,6-diamidino-2-phenylindole (DAPI, Sigma). Images were acquired with a DeltaVision wide-field deconvolution microscope (Applied Precision Inc., WA, USA), as previously described[44].

For live-cell and time-lapse imaging, HeLa cells were cultured in a glass-bottomed culture dish (MatTek, MA). During imaging, cells were maintained in CO_2-independent media (Invitrogen) containing 10% FBS and 1% glutamine in a sealed chamber at 37°C. Images of living cells were taken with a DeltaVision microscopy system at 1 frame per 5 sec. Images were prepared for publication using Photoshop (Adobe). Measurements and statistical analyses were performed using Image-Pro Plus 6.0 and GraphPad Prism. Statistical significance was determined by Student's t-test.

Microtubule plus-end tracking in live cells. To analyze the microtubule plus-end dynamics and generate kymography, we used ImageJ program (under the segmented line selections) to track the plus-end over the time. The related parameters such as duration for growth and pause, catastrophic and rescue frequency were generated by the program. An example of corresponding analysis was shown as supplementary Fig. S4.

Migration assay. For assay of wound healing, confluent MDA-MB-231 cells transfected with indicated siRNAs and placed on coverslips were scratched with a 20-μl pipette tip, then stimulated by 20% serum at 37°C for indicated times. Images were taken with a 10 × objective of an inverted microscope (Axiovert 200) coupled to an Axiocam-HS digital camera (Carl Zeiss, Germany). The relative healing velocities were measured using ImageJ software (NIH).

For single cell tracking, cells transfected with indicated shRNAs and/or indicated plasmids were starved overnight and then stimulated with 20% serum. Images were taken with a 20 × objective of a DeltaVision microscopy system (Applied Precision Inc.) at a rate of 1 frame/10 min. Cell movements were tracked by Image-Pro Plus 6.0. Total migration velocities (V_T) were total track distance divided by total time, and directional migration velocities (V_D) were the direct distance from start to end point divided by total time. Statistical significance was determined by Student's t-test.

***In vitro* plus-end tracking assay.** Assay for plus-end tracking was performed as described recently[46], with some modifications. The GMPCPP MT seeds were prepared by polymerizing 50 μM tubulin (at a bovine tubulin: rhodamine-tubulin: biotin-tubulin ratio of 30 : 2 : 1) in the presence of 1 mM GMPCPP (Jena Bioscience, Germany) at 37°C for 40 min. The seeds were then centrifuged and re-suspended in BRB80 buffer (80 mM K-PIPES, pH 6.8; 2 mM $MgCl_2$; and 1 mM EGTA) supplemented with 1 mM GMPCPP. Before use, these were sheared with a 35-guage needle to generate short seeds.

Flow chambers were prepared as described previously[47]. Chambers were coated with 10% monoclonal anti-biotin antibody (Sigma) followed by blocking with 5% Pluronic F-127 (Sigma). After a brief wash, sheared MT seeds (125 nM) were added into the chamber. Tubulin polymerization mixture (15 μM 1 : 30 rhodamine-labeled bovine tubulin in BRB80 buffer, 50 mM KCl, 5 mM DTT, 1.25 mM Mg-GTP, 0.25 mg/ml κ-casein, 0.15% methylcellulose (Sigma), an oxygen-scavenging system, and +TIPs) was introduced into the chamber to initiate polymerization. Unless stated otherwise, the final concentrations of +TIPs were 300 nM EB1 and 100 nM DDA3 deletion mutants. The temperature was maintained at 25°C. Images were collected with a super-resolution microscope configured on an ELYRA system (Carl Zeiss). The laser intensities were kept at a low level to avoid photobleaching. For +TIPs tracking assays, 1 frame was taken per second. Plus-end tracking of His GFP-DDA3 mutants was analyzed by use of kymographs in ImageJ software (NIH).

1. Watanabe, T., Noritake, J. & Kaibuchi, K. Regulation of microtubules in cell migration. *Trends Cell Biol* **15**, 76–83 (2005).
2. Mitchison, T. & Kirschner, M. Dynamic instability of microtubule growth. *Nature* **312**, 237–42 (1984).
3. Schuyler, S. C. & Pellman, D. Microtubule "plus-end-tracking proteins": The end is just the beginning. *Cell* **105**, 421–4 (2001).
4. Akhmanova, A. & Steinmetz, M. O. Tracking the ends: a dynamic protein network controls the fate of microtubule tips. *Nat Rev Mol Cell Biol* **9**, 309–22 (2008).
5. Carvalho, P., Tirnauer, J. S. & Pellman, D. Surfing on microtubule ends. *Trends Cell Biol* **13**, 229–37 (2003).
6. Galjart, N. & Perez, F. A plus-end raft to control microtubule dynamics and function. *Curr Opin Cell Biol* **15**, 48–53 (2003).
7. Komarova, Y. *et al.* EB1 and EB3 control CLIP dissociation from the ends of growing microtubules. *Mol Biol Cell* **16**, 5334–45 (2005).
8. Askham, J. M., Vaughan, K. T., Goodson, H. V. & Morrison, E. E. Evidence that an interaction between EB1 and p150(Glued) is required for the formation and maintenance of a radial microtubule array anchored at the centrosome. *Mol Biol Cell* **13**, 3627–45 (2002).
9. Galjart, N. Plus-end-tracking proteins and their interactions at microtubule ends. *Curr Biol* **20**, R528–37 (2010).
10. Jiang, K. *et al.* TIP150 interacts with and targets MCAK at the microtubule plus ends. *EMBO Rep* **10**, 857–65 (2009).
11. Honnappa, S., John, C. M., Kostrewa, D., Winkler, F. K. & Steinmetz, M. O. Structural insights into the EB1-APC interaction. *EMBO J* **24**, 261–9 (2005).
12. Honnappa, S. *et al.* An EB1-binding motif acts as a microtubule tip localization signal. *Cell* **138**, 366–76 (2009).
13. Bulinski, J. C. & Gundersen, G. G. Stabilization of post-translational modification of microtubules during cellular morphogenesis. *Bioessays* **13**, 285–93 (1991).
14. Siegrist, S. E. & Doe, C. Q. Microtubule-induced cortical cell polarity. *Genes Dev* **21**, 483–96 (2007).
15. Akhmanova, A. *et al.* Clasps are CLIP-115 and −170 associating proteins involved in the regional regulation of microtubule dynamics in motile fibroblasts. *Cell* **104**, 923–35 (2001).
16. Mimori-Kiyosue, Y. *et al.* CLASP1 and CLASP2 bind to EB1 and regulate microtubule plus-end dynamics at the cell cortex. *J Cell Biol* **168**, 141–53 (2005).
17. Fukata, M. *et al.* Rac1 and Cdc42 capture microtubules through IQGAP1 and CLIP-170. *Cell* **109**, 873–85 (2002).
18. Etienne-Manneville, S. & Hall, A. Cdc42 regulates GSK-3beta and adenomatous polyposis coli to control cell polarity. *Nature* **421**, 753–6 (2003).
19. Kroboth, K. *et al.* Lack of adenomatous polyposis coli protein correlates with a decrease in cell migration and overall changes in microtubule stability. *Mol Biol Cell* **18**, 910–8 (2007).
20. Kodama, A., Karakesisoglou, I., Wong, E., Vaezi, A. & Fuchs, E. ACF7: an essential integrator of microtubule dynamics. *Cell* **115**, 343–54 (2003).
21. Wen, Y. *et al.* EB1 and APC bind to mDia to stabilize microtubules downstream of Rho and promote cell migration. *Nat Cell Biol* **6**, 820–30 (2004).
22. Kumar, P. *et al.* GSK3beta phosphorylation modulates CLASP-microtubule association and lamella microtubule attachment. *J Cell Biol* **184**, 895–908 (2009).
23. Lo, P. K. *et al.* Identification of a novel mouse p53 target gene DDA3. *Oncogene* **18**, 7765–74 (1999).
24. Jang, C. Y. *et al.* DDA3 recruits microtubule depolymerase Kif2a to spindle poles and controls spindle dynamics and mitotic chromosome movement. *J Cell Biol* **181**, 255–67 (2008).
25. Hsieh, P. C. *et al.* p53 downstream target DDA3 is a novel microtubule-associated protein that interacts with end-binding protein EB3 and activates beta-catenin pathway. *Oncogene* **26**, 4928–40 (2007).
26. Miller, S. J. *et al.* Large-scale molecular comparison of human schwann cells to malignant peripheral nerve sheath tumor cell lines and tissues. *Cancer Res* **66**, 2584–91 (2006).
27. Bu, W. & Su, L. K. Characterization of functional domains of human EB1 family proteins. *J Biol Chem* **278**, 49721–31 (2003).
28. Mimori-Kiyosue, Y., Shiina, N. & Tsukita, S. Adenomatous polyposis coli (APC) protein moves along microtubules and concentrates at their growing ends in epithelial cells. *J Cell Biol* **148**, 505–18 (2000).
29. Jiang, K. *et al.* A Proteome-wide screen for mammalian SxIP motif-containing microtubule plus-end tracking proteins. *Curr Biol* **22**, 1800–7 (2012).
30. Vaughan, K. T. TIP maker and TIP marker; EB1 as a master controller of microtubule plus ends. *J Cell Biol* **171**, 197–200 (2005).
31. Komarova, Y. *et al.* Mammalian end binding proteins control persistent microtubule growth. *J Cell Biol* **184**, 691–706 (2009).
32. Xia, P. *et al.* EB1 acetylation by P300/CBP-associated factor (PCAF) ensures accurate kinetochore-microtubule interactions in mitosis. *Proc Natl Acad Sci U S A* **109**, 16564–9 (2012).
33. Zhang, L. & Yao, X. DDA3: A new dancer at the growing end? *Cell Cycle* **9** (2010).
34. Buey, R. M. *et al.* Sequence Determinants of a Microtubule Tip Localization Signal (MtLS). *J Biol Chem* **287**, 28227–42 (2012).
35. Moore, A. T. *et al.* MCAK associates with the tips of polymerizing microtubules. *J Cell Biol* **169**, 391–7 (2005).
36. Jaworski, J., Hoogenraad, C. C. & Akhmanova, A. Microtubule plus-end tracking proteins in differentiated mammalian cells. *Int J Biochem Cell Biol* **40**, 619–37 (2008).
37. Levy, J. R. & Holzbaur, E. L. Special delivery: dynamic targeting via cortical capture of microtubules. *Dev Cell* **12**, 320–2 (2007).
38. Watanabe, T. *et al.* Interaction with IQGAP1 links APC to Rac1, Cdc42, and actin filaments during cell polarization and migration. *Dev Cell* **7**, 871–83 (2004).
39. Lansbergen, G. *et al.* CLASPs attach microtubule plus ends to the cell cortex through a complex with LL5beta. *Dev Cell* **11**, 21–32 (2006).
40. Tsvetkov, A. S., Samsonov, A., Akhmanova, A., Galjart, N. & Popov, S. V. Microtubule-binding proteins CLASP1 and CLASP2 interact with actin filaments. *Cell Motil Cytoskeleton* **64**, 519–30 (2007).
41. Watanabe, T. *et al.* Phosphorylation of CLASP2 by GSK-3beta regulates its interaction with IQGAP1, EB1 and microtubules. *J Cell Sci* **122**, 2969–79 (2009).
42. Goh, L. K., Huang, F., Kim, W., Gygi, S. & Sorkin, A. Multiple mechanisms collectively regulate clathrin-mediated endocytosis of the epidermal growth factor receptor. *J Cell Biol* **189**, 871–83 (2010).
43. Choi, E. *et al.* BRCA2 fine-tunes the spindle assembly checkpoint through reinforcement of BubR1 acetylation. *Dev Cell* **22**, 295–308 (2012).
44. Zhang, L. *et al.* PLK1 phosphorylates mitotic centromere-associated kinesin and promotes its depolymerase activity. *J Biol Chem* **286**, 3033–46 (2011).
45. Yao, X., Abrieu, A., Zheng, Y., Sullivan, K. F. & Cleveland, D. W. CENP-E forms a link between attachment of spindle microtubules to kinetochores and the mitotic checkpoint. *Nat Cell Biol* **2**, 484–91 (2000).
46. Bieling, P. *et al.* Reconstitution of a microtubule plus-end tracking system in vitro. *Nature* **450**, 1100–5 (2007).
47. Dixit, R. & Ross, J. L. Studying plus-end tracking at single molecule resolution using TIRF microscopy. *Methods Cell Biol* **95**, 543–54 (2010).

Acknowledgements

This work is supported by Chinese 973 Project Grants 2010CB912103, 2012CB945002, 2013CB911203, and 2002CB713700; Chinese Academy of Science Grant KSCX2-YW-H-10; Anhui Province Key Project Grant 08040102005; International Collaboration Grant 2009DFA31010; Chinese Natural Science Foundation Grants 90508002, 91129714, and 90913016; MOE20113402130010; the Fundamental Research Funds for Central Universities (WK2060190018 and WK2340000021).and National Institutes of Health Grants DK56292, CA164133, and G12RR03034. X.Y. is a Cheung Kong Scholar.

Author contributions

Design of study: L.Z., H.S., P.X., G.F. and X.Y.; Experiments: L.Z., H.S., P.X., L.L., Z.W., T.Z., M.Y. and D.W.; Data analysis: L.Z., H.S., P.X., Z.W., Z.C., G.F. and X.Y.; Manuscript write-up: L.Z., H.S., D.H. and X.Y.

Additional information

Supplementary information accompanies this paper at http://www.nature.com/scientificreports

Competing financial interests: The authors declare no competing financial interests.

How to cite this article: Zhang, L. *et al*. DDA3 associates with microtubule plus ends and orchestrates microtubule dynamics and directional cell migration. *Sci. Rep.* **3**, 1681; DOI:10.1038/srep01681 (2013).